Eur. Phys. J. D **42**, 287–298 (2007)
DOI: 10.1140/epjd/e2007-00031-y

THE EUROPEAN PHYSICAL JOURNAL D

Experiments on the reflection of cold atoms from magnetic thin films

From atom optics to measurement of short-range forces

A.K. Mohapatra[a], S. Chaudhuri, S. Roy, and C.S. Unnikrishnan

Fundamental Interactions Laboratory (Gravitation Group), Tata Institute of Fundamental Research, Homi Bhabha Road, Mumbai-400 005, India

Received 20 August 2006 / Received in final form 5 December 2006
Published online 16 February 2007 –

Abstract. We report the results from a series of experiments in which ferromagnetic thin films were used as atom mirrors for laser-cooled rubidium atoms released from a magneto-optical trap. The thin films were made of cobalt and lanthanum calcium manganite (LCMO) with thicknesses between 20 and 300 nm. The magnetic domains in these thin films have a periodic structure where the spatial period is of the order of the thickness of the film, and the field decays exponentially above the film over a length scale comparable to the domain size. Thus, the neutral atoms reflect off these films from distances comparable to the thickness of the film, resulting in modification of the reflectivity due to the competition between the repulsive magnetic force and the attractive short-range forces such as van der Waals and Casimir forces. The smoothness of the atom mirror is also modified due to the proximity of the magnetic domains. The reflectivity is sensitive to the domain structure and size, which can be modified in LCMO by applying a modest external magnetic field. In this paper, we discuss the evaluation of the thin films as magnetic mirrors for atom optics, and the measurement of the van der Waals force with an accuracy of about 15%, using cobalt thin films. We also discuss some preliminary results on the temperature-dependent reflectivity for atoms near the ferromagnetic transition at 250 K in the LCMO film, and on the domain dynamics and relaxation.

PACS. 03.75.Be Atom and neutron optics – 32.80.Pj Optical cooling of atoms; trapping – 34.50.Dy Interactions of atoms and molecules with surfaces; photon and electron emission; neutralisation of ions – 75.70.-i Magnetic properties of thin films, surfaces, and interfaces

1 Introduction

Laser-cooled neutral atoms and Bose-Einstein condensates have emerged as convenient and sophisticated tools for a multitude of experiments and measurements pertaining to fundamental physics as well as applications. Developments in laser cooling and trapping, atom optics and atom interferometry have made atomic samples and beams highly versatile and flexible, surpassing the role of light in some areas, as probes and tools for precision experiments. The development of various atom-optical elements is an integral part of this progress.

In this paper, we focus on reflective mirrors for cold atoms based on ferromagnetic thin films, and discuss the measurements undertaken to evaluate magnetic thin films as atom mirrors for atom optics, and the experiments that exploit their novel properties for measurement of the van der Waals force on atoms in their ground state near a conducting surface [1]. Since the properties of ferromagnetic thin films made of various materials are of particular interest to condensed-matter physics, we also discuss some preliminary results on using atom-optics techniques to obtain information on the ferromagnetic transition, microscopic domain dynamics, and domain relaxation to equilibrium [2].

An atom mirror is the most basic component for atom optics, and much effort has been spent during the past two decades to develop and improve atom mirrors for reflecting cold atoms. Atom mirrors have been realised by creating repulsive interaction potentials either through electric-dipole coupling with a blue detuned evanescent wave [3–5] or magnetic-dipole coupling with an exponentially attenuated magnetic field created above a surface with an alternating magnetic pattern [6,7]. Both types of atom mirror have been used as basic tools for the precision measurement of atom-surface interaction [1,8]. Magnetic atom mirrors have some advantages over the evanescent-wave atom mirrors due to the absence of any perturbation

[a] e-mail: a.k.mohapatra@durham.ac.uk

from spontaneous emission, and due to their passive stability. In addition, surface engineering can be performed with great flexibility, in various shapes over large areas, unlike cases in which an evanescent optical field is used.

The magnetic atom mirror for cold atoms was first proposed by Opat et al. [6], and employed a periodic magnetic structure. The magnitude of the magnetic field above a periodic magnetic structure decreases exponentially, with a decay constant related to the magnetisation periodicity. An atom in a magnetic field of magnitude B has a magnetic dipole interaction energy $U = -\mu_\zeta B$, where μ_ζ is the projection of its magnetic moment onto the field direction. In the case of experiments with slow atoms, the magnetic moment of the atoms follows the field direction adiabatically. In the regime of adiabaticity and the linear Zeeman effect (when the field is less than about 300 G), ^{85}Rb atoms in the positive $m_F g_F$ states are repelled by the quantised Stern-Gerlach force $(-\nabla U)$ arising from the strong gradient of the magnetic field above the surface. Magnetic atom mirrors have been realised by making the magnetisation alternate in sign on an audio tape [9], floppy disk [10], video tape [11], using array of permanent magnets [12], array of current carrying wires [13], cobalt single crystal [14] and fabricated magnetic microstructures [15,16]. These mirrors are mostly used in modern atom optics where high reflectivity and smoothness are desired.

In this article, we report on several experiments that employ a new kind of magnetic atom mirror made of magnetic thin films [1,2]. Ferromagnetic thin films have naturally periodic patterns of alternating magnetisation, in the form of stripes of magnetic domains, with periodicity on the order of the thickness of the film. Even though these domains are not parallel and straight over large length scales, their alternating nature over small scales makes them physically resemble the periodic magnetisation pattern present in structured artificial magnetic atom mirrors. The magnetic field decays exponentially over the surface of the film, with a decay length comparable to the thickness of the film. Therefore, good reflectivity for cold atoms with a magnetic moment is expected when relatively thick films are used as mirrors, in which case the attractive atom-surface force is negligible. For thin films, with thicknesses of about 100 nm or less, the closest approach of the atoms to the surface before reflection is also about 100 nm or less, and the atom-surface force becomes appreciable. The surface field of such a thin film is about 2 kG and the gradient is sufficient to compete with the attractive atom-surface interaction to reflect a significant fraction of the atoms. Due to the proximity to the magnetic domains, the field and thus the mirror are highly corrugated, which increases the divergence of the reflection, although such mirrors are suitable for the precision measurement of atom-surface interactions such the Casimir-Polder and the van der Waals force. We discuss two kinds of thin films (cobalt and $La_{0.7}Ca_{0.3}MnO_3$ (LCMO)) that are used as magnetic atom mirrors. When the film thickness is larger than 200 nm or so, the mirror reflectivity is close to 100%, but the divergence is about

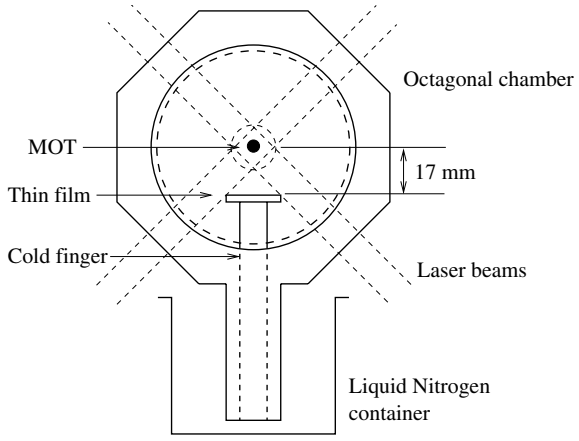

Fig. 1. Schematic of the MOT setup. The thin film used as the atom mirror is mounted 17 mm below the MOT centre on a cold finger cooled by liquid nitrogen.

20 times greater than that measured with the smoothest magnetic atom mirrors. As the thickness of the film decreases, the reflectivity is reduced due to the attractive van der Waals force, and this allows a relatively precise measurement of the atom-surface interaction potentials that are dependent on spin. We have thus measured the van der Waals force with a precision of 15%, and the measured value of the C_3 coefficient agrees well with recent theoretical estimates [2].

We have studied the reflectivity of cold atoms from LCMO thin films because of their interesting magnetic properties. LCMO thin films are of great interest in condensed-matter research, especially in the context of their magneto-resistive properties. Apart from a ferromagnetic transition at a temperature easily accessible with even thermoelectric coolers, LCMO has a relatively small coercive field, making its domain pattern and dynamics sensitive to external fields that can be easily applied in cold-atom experiments. Furthermore, thin films of good quality can easily be made with large areas, and their properties are well characterised. These experiments were performed using thin films mounted on a cold finger (cooled by liquid nitrogen) inside a vacuum chamber. We report some preliminary results on the observation of the temperature-dependent magnetic phase transition, relaxation, and dynamics of the magnetic domains in the LCMO thin film.

2 Experimental details

2.1 The cold-atom source

We use a magneto-optical trap (MOT) as our cold-atom source. The MOT setup is described in detail in reference [2]. A schematic of our MOT setup is shown in Figure 1. The MOT was formed in an SS octagonal chamber equipped with glass viewports and evacuated to less than 5×10^{-10} torr. Rubidium atoms (^{85}Rb) were loaded into the MOT from a vapour at a background pressure less

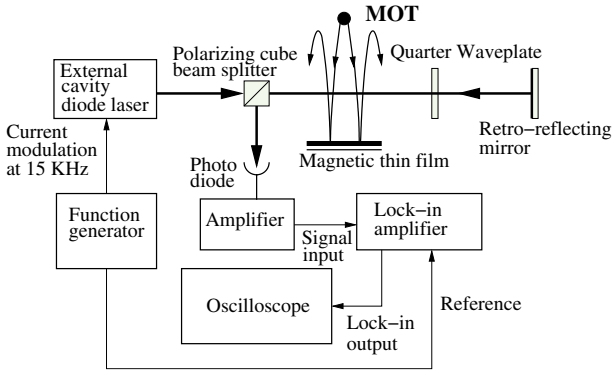

Fig. 2. Schematic of the atomic-reflection experiment.

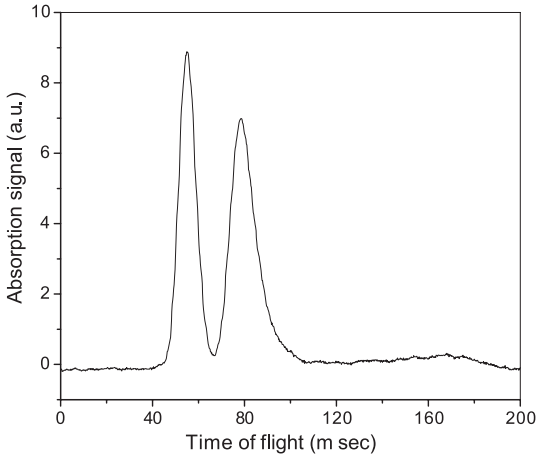

Fig. 3. Time-of-flight signal of atoms prepared in the $F_g = 3$, $m_F = +3$ state bouncing from the cobalt thin film of thickness 180 nm. The absorption peak observed at about 60 ms is due to the atoms falling through the probe, and the peak observed at about 80 ms is due to the atoms passing through the probe after reflection from the mirror. A weak absorption peak is observed at about 170 ms, and is due to the reflected atoms falling through the probe beam again.

than 1×10^{-9} torr for about 10 seconds in order to obtain a cold atomic cloud of up to 10^7 atoms. A quadrupole field of gradient 6 G/cm for the MOT was generated by a pair of coils in an anti-Helmholtz configuration, located close to the chamber. Two external cavity diode lasers (Toptica DL100) with spectral width less than 1 MHz, and working at 780 nm, were used for the MOT. The cooling-laser frequency was locked at 13 MHz red-detuned to the $5S_{1/2}\ F_g = 3 \longrightarrow 5P_{3/2}\ F_e = 4$ transition. The re-pump laser was locked to the $5S_{1/2}\ F_g = 2 \longrightarrow 5\ P_{3/2}\ F_e = 3$ transition. The cooling and re-pump beams were expanded to a Gaussian width of 10 mm, and the power in each cooling beam was about 5 mW. After loading the MOT for about 10 seconds, the cooling-beam frequency was red-detuned by 50 MHz from the cooling transition, and the intensity was reduced using the acousto-optic modulator to further cool the atoms in the optical molasses. The quadrupole field was kept switched off during the molasses phase, and the residual fields were cancelled by using three pairs of large Helmholtz coils around the chamber. With about 15 ms of molasses phase, the atoms were cooled to a temperature of about 10 μK.

2.2 Atomic-reflection experiment

A schematic of the experimental setup along with the essential electronics is shown in Figure 2. Cold atoms at a temperature of about 10 μK (r.m.s. velocity of about 3 cm/s) were released onto the thin film atom mirror kept 17 mm below the cloud, by switching off the MOT laser beams. During the release, the re-pump beam was left on to ensure that all of the atoms remained in the $F_g = 3$ state. The r.m.s. size of the slowly expanding atomic cloud becomes about 3 mm at the surface of the mirror, which has dimensions of 1 cm $\times$ 1 cm. Thus, about 99% of the atoms in the cloud interact with the thin-film atom mirror. Experiments were performed with unpolarised atoms as well as with spin-polarised atoms. To achieve spin-polarisation, the atoms were optically pumped into the $F_g = 3, m_F = 3$ ($F_g = 3, m_F = -3$) state by irradiating a retro-reflected σ^+ (σ^-) laser beam resonant to the $5S_{1/2}\ F_g = 3 \longrightarrow 5P_{3/2}\ F_e = 3$ transition in a constant bias field of about 1 G in the laser beam propagation direction, before the atoms interacted with the mirror.

The atoms were detected by a weak probe laser beam (about 2 μW), resonant to the $5S_{1/2}\ F_g = 3 \longrightarrow 5P_{3/2}\ F_e = 4$ transition, and kept between the MOT centre and the mirror. The probe beam had a horizontal profile with uniform intensity over a rectangular area of 20 mm $\times$ 0.5 mm. This was retro-reflected and sent to a photo-diode using a polarising-cube beam splitter and a quarter-wave plate to detect the absorption. The frequency of the probe beam was modulated by modulating the current to the laser at 15 kHz. The absorption of the probe intensity was detected by a photo-diode and a low-noise amplifier feeding into a lock-in amplifier, with its reference derived from the laser current modulation. We have achieved a sensitivity for detecting a few hundred atoms in the probe beam using this phase-sensitive technique [17]. The reflection of cold atoms from the mirror was monitored by observing the time-of-flight (TOF) signal. A typical TOF signal observed in the atomic-reflection experiment is shown in Figure 3.

3 Cobalt thin-film atom mirror

Cobalt thin films possess stripe-like domain patterns, with out-of-plane magnetisation [18]. The domain pattern of a cobalt thin film of thickness 180 nm, as determined by magnetic-force microscopy (MFM), is shown in Figure 4. The magnetic field above the surface of the cobalt thin film can be calculated by approximating the domain pattern by parallel stripes of magnetisation, alternating in sign. The magnetic field above an array of magnets with magnetisation alternating in sign and infinite thickness is

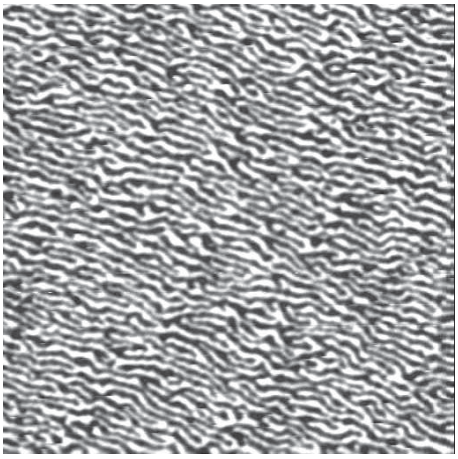

Fig. 4. Magnetic-force microscopy (MFM) image of a cobalt thin film of thickness 180 nm. The scanned area is about 10 μm $\times$ 10 μm. The domain periodicity is about 282 nm.

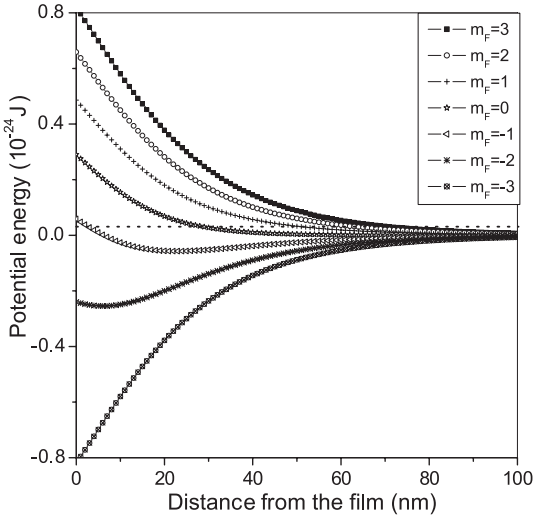

Fig. 5. The potential experienced by the atoms in the different Zeeman states due to their interaction with the magnetic field above a cobalt thin film of thickness 45 nm. The dotted line is the kinetic energy of the atoms at the mirror surface.

discussed in reference [16] and is given by

$$B_x(x,y) - iB_y(x,y) = B_0 \ln\left[\frac{1+e^{-2\pi(y-ix)/a}}{1-e^{-2\pi(y-ix)/a}}\right], \quad (1)$$

where the x-axis is in the direction of magnetic periodicity and the y-axis is perpendicular to the mirror surface. B_0 is the magnetic field at the mirror surface and $a/2$ is the width of a magnet in the array. The magnitude of the magnetic field at the centre of a magnet is then

$$B(y) = B_0 \tan^{-1}\left[e^{-2\pi y/a}\right]. \quad (2)$$

Equation (2) can be derived by considering only the first Fourier component of the field pattern of the periodic array of magnets. For the magnetic atom mirror, the higher Fourier components decay much faster [7] than the first Fourier component, and hence can be neglected. So, equation (2) is a good approximation for calculating the magnitude of the magnetic field above any point on the mirror.

The magnitude of the magnetic field above the cobalt thin film can be determined from equation (2) with the finite-thickness correction, which can be included as described in reference [7]. The magnitude of the magnetic field at a distance y above the cobalt thin film can be approximated by

$$B(y) = B_0\left(\tan^{-1}\left[e^{-2\pi y/\lambda(d)}\right] - \tan^{-1}\left[e^{-2\pi(y+d)/\lambda(d)}\right]\right), \quad (3)$$

where $\lambda/2$ is the width of a domain and d is the thickness of the film. The surface field of cobalt is expected to be a few kG, and hence the quadratic Zeeman effect becomes important very close to the surface. For a high magnetic field, the magnetic interaction potential for alkali atoms in various magnetic sub-levels can be calculated using the Breit-Rabi formula [19]. The magnetic interaction potential above the cobalt thin film of thickness 45 nm for ^{85}Rb atoms in various magnetic states of the ground state $F_g = 3$ is shown in Figure 5. Atoms in a magnetic state with kinetic energies less than the corresponding barrier height are reflected back from the atom mirror. As shown in Figure 5, the magnetic interaction potentials for atoms in states other than the $m_F = -3$, -2 states are reflective. However, for a higher surface field, the magnetic potential for atoms in the $m_F = -2$ state can also be reflective, although the potential for the atoms in the $m_F = -3$ state is always attractive.

In the experiment, cobalt thin films of four different thicknesses — 180 nm, 90 nm, 45 nm, and 20 nm — were used as atom mirrors. The films were prepared on silicon substrates by dc magnetron sputtering. The surface topography was determined from atomic-force microscopy, and the local roughness was found to be less than 1 nm. The saturation magnetic field was estimated to be larger than 1 kG by measuring the B-H curves in a superconducting quantum interference device (SQUID) magnetometer. The domain patterns of the films were observed by magnetic-force microscopy (MFM), and the films were found to possess stripe-like domain patterns with out-of-plane magnetisation, as shown in Figure 4. The fluctuation in the domain periodicity is about 14%, as measured from the MFM image. The thickness was calibrated by growing the films on partially covered silicon substrates, and the resulting step was measured in a DEKTAK profilometer.

The reflection of atoms from the cobalt thin-film atom mirror was observed as described in Section 2. The TOF signal of the cold atoms (prepared in the $F_g = 3, m_F = +3$ state) bouncing from a cobalt thin film of thickness 180 nm is shown in Figure 3. Reflection of the unpolarised atoms from the mirror is also observed, and the reflectivity is lower than in the case of spin-polarised atoms. The reflection of atoms prepared in the $F_g = 3, m_F = -3$ state is less than 5% (instead of zero), indicating a small amount of spin-flipping near the mirror. This could also indicate a slight imperfection in spin-polarisation. The

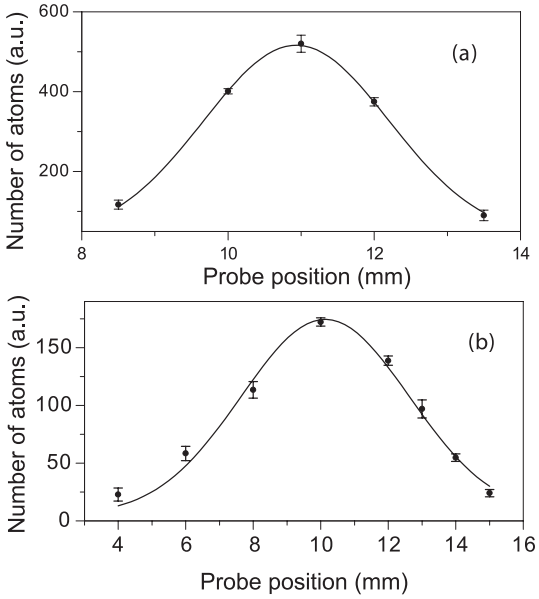

Fig. 6. Spatial profiles of the (a) incident and (b) reflected atomic clouds. Circles show the experimental data while the solid lines are the Gaussian fittings.

characterisation of the cobalt thin-film atom mirror is presented in the following section.

3.1 Corrugation of cobalt thin-film atom mirror

The magnetic equipotential surfaces close to the surface of the cobalt thin-film atom mirror may be rough close to its surface due to the presence of the higher harmonics in the periodic pattern of the magnetisation. The presence of the components of the bias field in the periodicity direction can enhance the effective corrugation and roughness. The corrugation of a magnetic atom mirror is discussed in detail in reference [7]. The roughness in the magnetic equipotential surface of the magnetic atom mirror results in non-specular reflection of the atoms from the mirror. The deviation of the reflection angle from that for specular reflection can be expressed as [7]

$$\theta_C = \frac{\Delta v_x}{v_0}, \tag{4}$$

where Δv_x is the change in the velocity parallel to the mirror surface and v_0 is the average vertical impact velocity of the atoms at the mirror.

For the magnetic thin-film atom mirror, the corrugation was determined by comparing the horizontal spatial profiles of the atomic cloud before and after reflection. Each spatial profile was measured by stepping a 1 mm diameter probe beam sequentially across the mirror in the horizontal direction at 7 mm above the mirror surface. The spatial profiles of the incident and reflected atomic clouds are shown in Figure 6. The x-scale in the upper graph is magnified by about 2.5 times compared to that in the lower graph. The change in the horizontal velocity (Δv_x) is calculated as $(\sigma_{exp} - \sigma_{spec})/t$, where σ_{exp} is the observed Gaussian radius of the reflected cloud, σ_{spec} is the Gaussian radius of the cloud for the specular reflection, and t is the time of propagation after reflection. σ_{exp} for the reflected cloud in Figure 6 is 3.5 mm. The propagation time is determined from the TOF signal, which is about 13 ms. σ_{spec} can be calculated from the formula $\sigma_{spec} = \sqrt{\sigma_0^2 + \frac{k_B T}{M} t_1^2}$, where σ_0 is the Gaussian radius of the initial atomic cloud and t_1 is the total time of propagation. In our experiment, for the atomic cloud at a temperature around 10 μK, σ_{spec} is 2.5 mm. From these data, the deviation of the reflection angle from the specular reflection was estimated to be 128 mrad. This is about 20 times more than that measured with the smoothest atom mirrors developed from magnetic video tapes [11]. A large amount of corrugation is expected in the case of a magnetic thin-film atom mirror, since the atoms approach very close to the surface.

3.2 Inelastic reflection of cold atoms

It can be seen from the experimental data that some atoms of the cold atomic cloud reflect inelastically. This inelasticity is demonstrated from the TOF signals observed by keeping the probe beam at different heights from the mirror's surface. As the height of the probe beam from the mirror's surface increases, the ratio of the absorption signals from the reflected and falling atoms decreases, as shown in Figure 7. In addition, the width of the absorption signal from the reflected atoms increases with increasing probe height from the film's surface, as shown in Figure 8 for the case of atoms reflecting from the cobalt thin film of thickness 180 nm. The use of a probe beam with a Gaussian width smaller than the cloud size could cause a similar observation. However, in our experiment, the probe beam has a constant intensity profile in the horizontal direction and is much wider than the reflected cloud size.

The observations in Figures 7 and 8 could be due to the large corrugation of the cobalt thin-film atom mirror. In the case of non-specular elastic reflection, atoms gain extra momentum in the horizontal direction after reflection. Since the atoms move through a static potential, the momentum of the reflected atoms in the direction of gravity is transferred in the horizontal direction due to energy conservation. Thus, in our experiment, non-specular elastic reflection could mimic inelastic reflection. However, the loss of momentum in the direction of gravity due to the corrugation is estimated to be an order of magnitude smaller than the momentum loss estimated from the measured inelasticity. Under our experimental conditions, and when considering the small correction due to the non-specular reflection of the atoms, the reflectivity should remain constant for the different probe heights above the mirror surface if the reflection of the cold atomic cloud is purely elastic, even with the corrugation present in the mirror. In addition, the widths of the reflected peak and the falling peak should remain the same after correcting for thermal expansion and for any heating effect due to

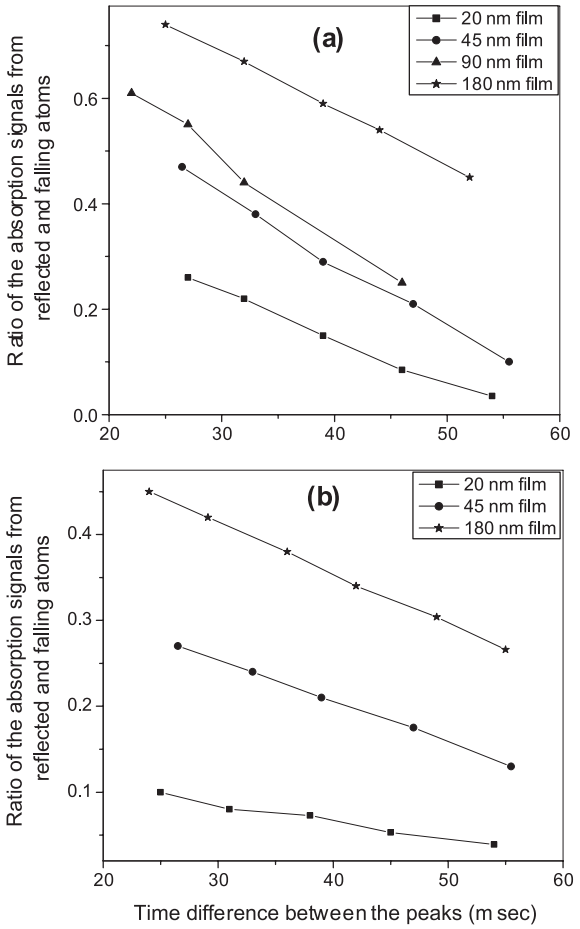

Fig. 7. Ratio of the absorption signals from reflected and falling atoms in the case of (a) spin-polarised, (b) unpolarised atoms reflecting from the thin films of different thickness. The x-axis denotes the time difference between the peaks, which is related to the height of the probe from the film's surface.

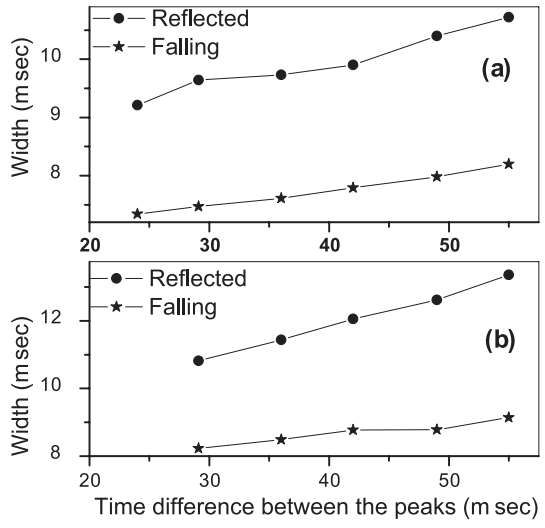

Fig. 8. Width of the absorption signals from the falling and reflected atoms in the case of (a) unpolarised and (b) spin-polarised atoms reflecting from a 180 nm thick film.

the interaction of the spin-polarised atoms with the probe light. However, the observed data point to some genuine inelastic reflection, and the number of atoms steadily decreases as the probe height is increased.

The observed inelasticity in the reflection can be modelled qualitatively by considering the spin-flipping of the atoms. The adiabatic condition for slowly moving neutral atoms in a magnetic field is discussed in reference [20], and for the magnetic thin-film atom mirror it can be expressed as

$$\frac{2\pi}{\lambda} v_y \left(\frac{|\mathbf{B}(y)|}{|\mathbf{B}(y) + \mathbf{B_G}|} \right) \ll \omega_l, \tag{5}$$

where v_y is the velocity of the atoms, $\mathbf{B_G}$ is the bias field, ω_l is the Larmor frequency of the atom, $\mathbf{B}(y)$ is the magnetic field above the film's surface, and λ is the periodicity of the magnetic domains. For the cobalt thin films used in our experiment, $\lambda \approx 100$ nm, and the adiabatic condition is not satisfied in some parts of the atomic trajectory where spin-flipping may occur. After reflection, atoms moving away from the magnetic mirror can flip to the lower m_F states and experience a lower potential. Thus, the atoms lose some of their kinetic energy. So, when the atoms are prepared in the $m_F = +3$ state, the atoms will flip to the lower m_F states and lose their kinetic energy on average and hence will slow down and reach a lesser height. As a result, the width of the reflected peak of the TOF signal increases and the peak height decreases with increasing probe height from the film's surface. It is observed that inelasticity in the case of unpolarised atoms is less than in the case of spin-polarised atoms. Since the atoms are distributed amongst all the Zeeman states in the case of unpolarised atoms, flipping to both higher and lower m_F states is possible, which is not the case for spin-polarised atoms. Hence, the average kinetic energy loss would be less in the case of unpolarised atoms.

3.3 Reflectivity of cobalt thin-film atom mirrors of different thickness

The thickness dependence of the reflectivity of cold atoms from the cobalt thin-film atom mirror was measured in our experiment, and the data were used to determine the coefficient of the van der Waals interaction potential of rubidium atoms near a cobalt surface. Due to the inelasticity in the reflection, determination of the reflectivity from the TOF signal, keeping the probe at a particular height from the mirror's surface, would underestimate the reflectivity. The true reflectivity can be determined by measuring the fraction of reflected atoms just above the film's surface, immediately after the bounce. TOF signals were observed at different probe heights from the mirror's surface in order to determine the variation of the ratio of the peak heights, and this is shown in Figure 7 for the spin-polarised and unpolarised atoms reflected from thin films of different thickness. Then, the ratio of the peak heights was extrapolated close to the film's surface in order to obtain the true reflectivity. The extrapolation towards the film's surface was done by fitting the straight lines to the observed

Table 1. Reflectivity of the spin-polarised cold atoms from cobalt thin films.

Film thickness (nm)	Reflectivity (%)	Error (%)
180	100	0.5
90	94.6	3.2
45	79.6	2
20	48.7	1.6

Table 2. Reflectivity of the unpolarised cold atoms from cobalt thin films (note: for the 90 nm film, we have only one data for the ratio of the absorption signals from the reflected and falling atoms for the probe beam at a height of 6 mm from the film's surface. In this case, interpolation using the data corresponding to the 45 nm and 180 nm thin films was also used to determine the reflectivity for the 90 nm thin film).

Film thickness (nm)	Reflectivity (%)	Error (%)
180	59	0.8
90	45.5	2.5
45	39.7	1
20	13.8	1.3

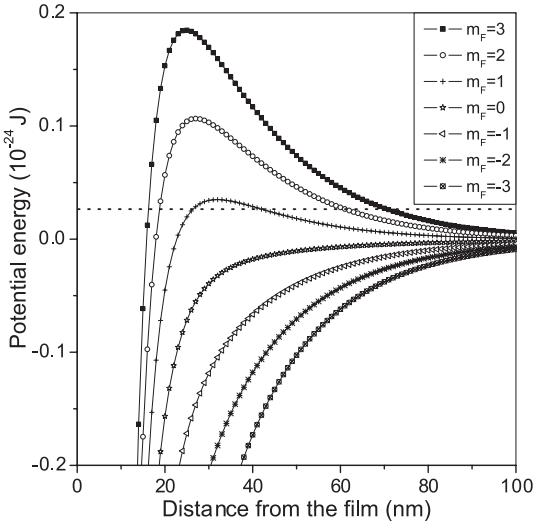

Fig. 9. The effective potential experienced by the atoms in different Zeeman sub-levels, including the van der Waals interaction with the magnetic interaction potential energy above a 45 nm thick film. The dotted line is the kinetic energy of the atoms at the mirror's surface.

experimental data. The errors in the reflectivity were determined from the statistical errors in the extrapolations. The reflectivity and the errors estimated for the reflection of spin-polarised and unpolarised atoms from cobalt thin films of different thicknesses are given in Tables 1 and 2 respectively.

4 Measurement of the van der Waals force

4.1 The effective interaction potential

Cobalt thin films have a characteristic stripe-like domain structure, which was predicted by Kittel [21], and the domain periodicity (λ) changes with the thickness of the film (d) and obeys the law $\lambda \propto \sqrt{d}$ [21]. The stripe-like domain pattern has been observed in single-crystal cobalt thin films grown by molecular beam epitaxy (MBE) [18]. The thin films used as atom mirrors in our experiment were prepared by dc magnetron sputtering. The domain pattern for a 180 nm thick film, observed using magnetic force microscopy (MFM), is shown in Figure 4. The domain patterns of these films are very similar to those in films prepared by MBE, except that the spread in the periodicity parameter is slightly larger. The domain periodicity is determined from the MFM image and the mean domain periodicity of the 180 nm thick film is about 282 nm, which is the same as the domain periodicity observed in the case of the MBE-grown cobalt thin films [18] to within 5%. Therefore, the observed domain periodicity as a function of thickness for the MBE-grown cobalt thin films (as given in Ref. [18]) has been used to calculate the magnetic field above the present cobalt thin films of different thicknesses.

In the case of thin-film atom mirrors of relatively small thickness, the closest approach of the atom is less than 100 nm. At this distance from the surface, the atom-surface attractive interaction becomes comparable to the repulsive magnetic potential. Retardation effects are relatively small at this distance. The effective potential is the sum of the repulsive magnetic interaction potential and the attractive van der Waals potential (C_3/z^3), which is shown in Figure 9. Close to the surface, the van der Waals attraction dominates over the magnetic repulsion, which results in a barrier peak in the intermediate range. Atoms in a magnetic state with kinetic energy less than the corresponding barrier peak are reflected from the mirror. With reference to Figure 9, atoms in the states $m_F = 3, 2, 1$ are reflected from the mirror. By comparing with Figure 5, one can see that the presence of the van der Waals interaction potential dramatically modifies the reflectivity, because of the competition with the magnetic repulsion, which is exploited in this experiment. The range of the magnetic interaction potential changes with the thickness of the film, and hence the thickness of the thin film is used as a variable parameter in order to measure the van der Waals coefficient.

4.2 Determination of the van der Waals coefficient

The measured data for the reflectivity of unpolarised cold atoms from the cobalt thin films of four different thicknesses are summarised in Table 2. This is used to determine the van der Waals coefficient by performing least-squares fitting with the numerically computed reflectivity as a function of thickness of the thin films. The van der Waals coefficient (C_3) and surface field (B_0) are taken to be the free parameters in the least-squares fitting. The cold atoms dropped from the optical molasses have

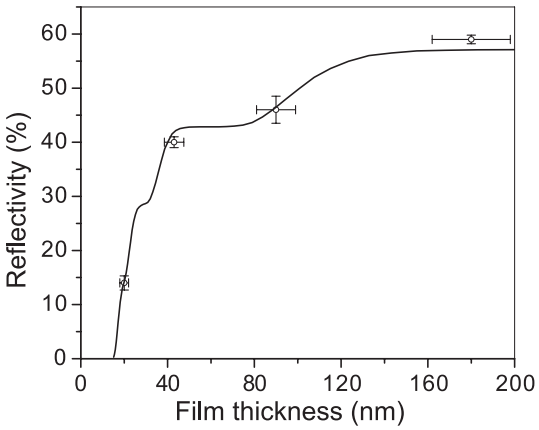

Fig. 10. Reflectivity of the unpolarised cold atoms as a function of thickness of cobalt thin films. Circles represent the experimental observations, while the solid line is the computed reflectivity using the van der Waals coefficient and the surface field determined from least-squares fitting.

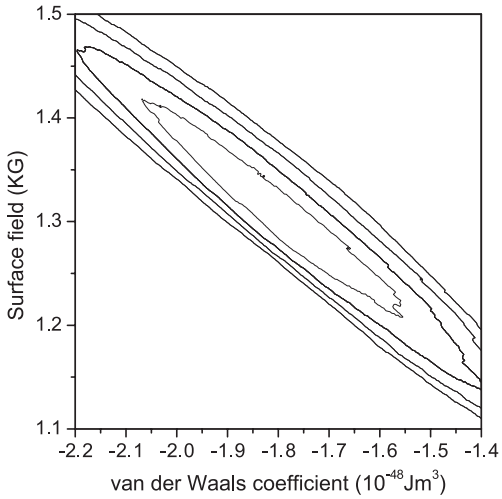

Fig. 11. χ^2 distribution of the fitting.

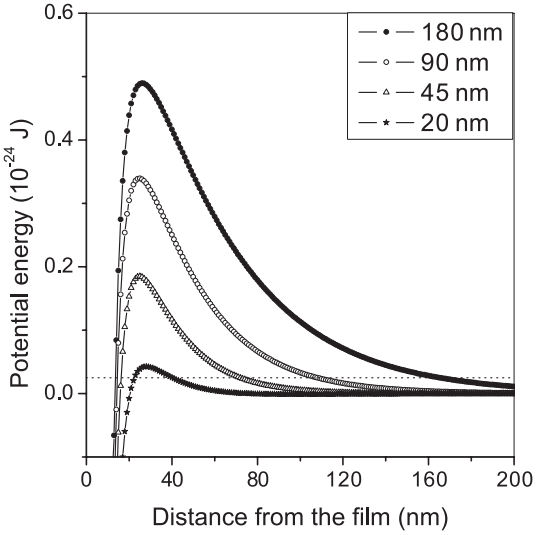

Fig. 12. The effective potential experienced by the atoms in the $F_g = 3, m_F = +3$ state above the four thin films used in our experiment. The dotted line represents the kinetic energy of the atoms at the mirror's surface.

a well-defined mean kinetic energy at the mirror's surface, and the spread in kinetic energy of the atoms due to the temperature of the cloud is less than 1% of the mean kinetic energy. Atoms in Zeeman sub-levels with kinetic energy less than the corresponding barrier peak of the effective potential are reflected back from the mirror. The reflectivity is calculated by assuming a uniform distribution of the atoms in all Zeeman sub-levels, since the atoms were released from the optical molasses without spin polarisation [22]. Since there are finite number of Zeeman sub-levels, reflectivity as a function of the thickness of the film is a multi-step (quantised) function. Including a small variance in the local surface field on the order of 10% makes the steps in the reflectivity function smooth. The fitted curve is shown in Figure 10 along with the experimental data. The best-fit values are 1.75×10^{-48} Jm^3 for the van der Waals coefficient, and 1.28 kG for the surface field. The measured value agrees well with the recent theoretical calculation of C_3 after including the finite conductivity of cobalt [2,23,24]. The χ^2 distribution of the fitting in the parameter space is shown in Figure 11. The closed contours of the χ^2 distribution shows the stability of the fitting.

The data obtained for the spin-polarised atoms were compared with their computed reflectivity using the same values of C_3 and B_0 as determined from the reflectivity data obtained for the unpolarised atoms. Atoms, spin-polarised in the state ($F_g = 3$, $m_F = +3$) should have experienced 100% reflection from all of the thin films used in our experiment, since the barrier heights of the effective potentials corresponding to the $m_F = +3$ state are more than the kinetic energy of the atoms for all of the thin films, as shown in Figure 12. However, a reduction in the reflectivity is observed in the experiment, as the thickness of the film is reduced, which is attributed to the spin-flip of the atoms from the $m_F = +3$ state to the other Zeeman states when they approach the mirror's surface. At the time of reflection from the mirror surface, the atoms are distributed over the different Zeeman states due to spin-flipping, although they are initially prepared in the $m_F = +3$ state. In order to compare the computed reflectivity from the model against the reflectivity of the spin-polarised atoms observed in the experiment, the change in the distribution of these spin-polarised atoms approaching the mirror's surface is approximately determined by considering the following observations. The effective potential for the 20 nm thin film is shown in Figure 13, and the reflectivity of the spin-polarised atoms from the 20 nm thin film is about 50%. Therefore, we estimate that about 50% of the atoms suffer spin-flip as they approach the 20 nm thin film. This is consistent with the entire data set if we take into account the fact that the probability of flipping to a nearer Zeeman state is higher. The reflectivity thus computed is used to compare with the experimentally observed reflectivity from all of the films [2]. The comparison

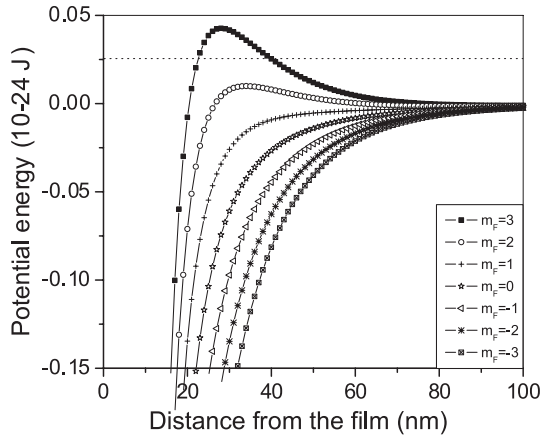

Fig. 13. The effective potential experienced by the atoms in different Zeeman sub-levels, including the van der Waals interaction with the magnetic interaction potential energy, above a 20 nm thick film. The dotted line represents the kinetic energy of the atoms at the mirror's surface.

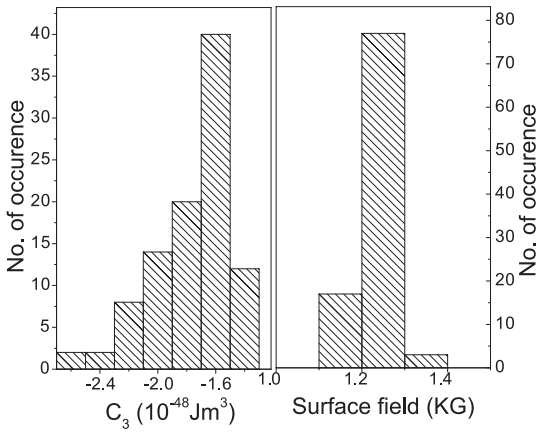

Fig. 15. Distribution of the coefficient of the van der Waals potential (C_3) and the surface field (B_0), determined from the Monte Carlo simulation. The error on (C_3) is 15% and on (B_0) is 12%.

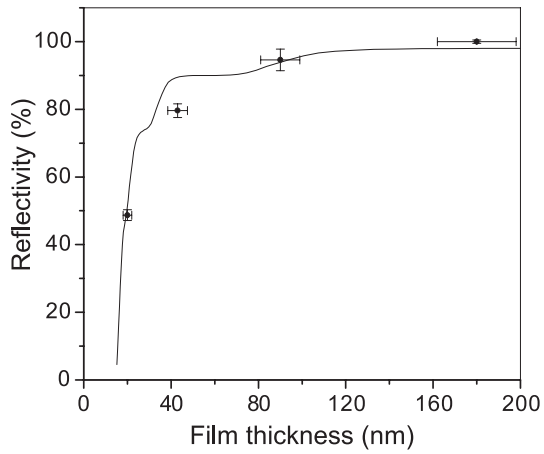

Fig. 14. Reflectivity of the spin-polarised cold atoms as a function of thickness of the cobalt thin film. Circles represents the experimental observations, while the solid line is the computed reflectivity using the van der Waals coefficient and the surface field, determined from the least-squares fitting.

is shown in Figure 14, and it can be seen that the model matches the data well.

4.3 Error on the van der Waals coefficient

The error in the van der Waals coefficient was determined by performing a Monte Carlo simulation. The statistical uncertainty determined from the repeated measurements was taken as the error in the reflectivity. The errors in the film thickness were determined from DEKTAK profilometer measurements. Random numbers with a Gaussian distribution around the mean value of the experimental data were generated by taking these errors as the Gaussian half-widths. The least-squares fitting was performed with the points generated from the Monte Carlo simulation in order to obtain the distributions of the parameters. The histograms representing the distributions of the parameters are shown in Figure 15. The 1σ estimate on the width of the distribution of the coefficient of the van der Waals potential is 15%, and that of the surface field is 12%, and these determine the uncertainties in the parameters. Including the 14% fluctuation in the domain periodicity doesn't appreciably change the best-fit values or the error of the van der Waals coefficient. However, the steps in the reflectivity function become less steep.

5 LCMO thin-film atom mirror

Lanthanum Calcium Manganite (LCMO) thin films exhibit a paramagnetic-to-ferromagnetic phase transition at about 250 K. The LCMO film grown on (001)-oriented single crystalline $LaAlO_3$ (LAO) substrate has a stripe-like domain pattern with out-of-plane magnetisation [25]. The surface field is on the order of a few kG [26]. The film has a coercive field on the order of 600 G when the magnetic field is applied parallel to the film's surface [26]. Hence, the reflectivity of the cold atoms from the LCMO thin-film atom mirror would be sensitive to a small applied magnetic field.

The LCMO thin films used in our experiment were grown on a LAO substrate in the (100) plane, using pulsed-laser deposition. The thickness of the film was 120 nm, as measured by a profilometer. The local roughness of the surface is about 30 nm, which was determined from atomic-force microscopy. The coercive field for the (100) film is known to be relatively lower, and is about 200 G in our case, as measured in a SQUID magnetometer. The film was mounted on a cold finger, which was cooled to 80 K using direct contact with liquid nitrogen in a small reservoir. The temperature of the film was measured using a calibrated platinum sensor kept in good thermal contact with the cold finger in close proximity

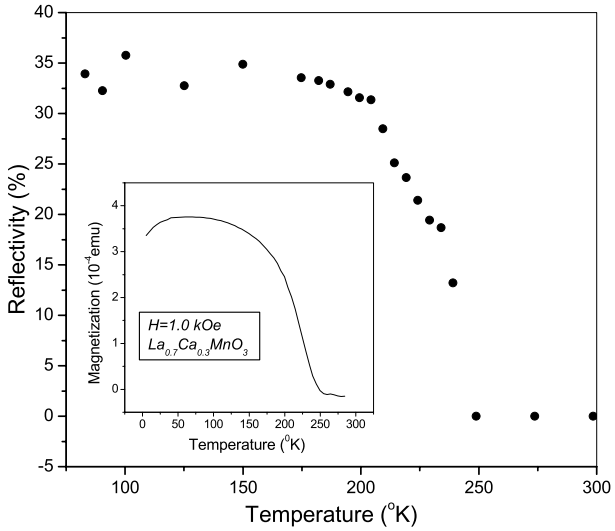

Fig. 16. Reflectivity of the spin-polarised cold atoms from the LCMO thin film as a function of temperature. The magnetisation measurement using the SQUID magnetometer as a function of temperature is shown in the inset.

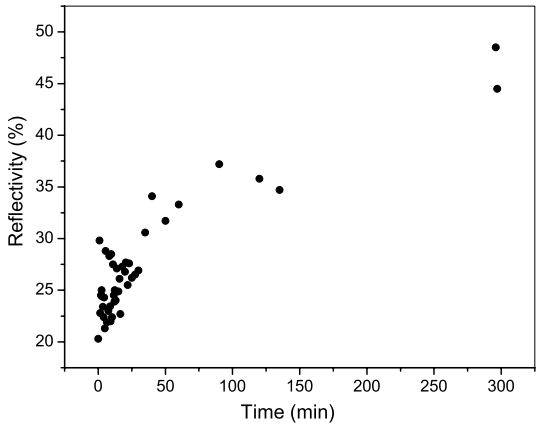

Fig. 17. Change in the reflectivity of cold atoms with time after magnetising the film in the direction parallel to the plane.

to the substrate. Due to the small coercive field, the reflectivity of the cold atoms from this film is sensitive to a small external magnetic field, which can easily be applied in our laser-cooling setup. This film possesses a domain pattern of in-plane magnetisation that is composed of several grains with sizes on the order of 500 nm [27]. The magnetic field above such a film is difficult to calculate due to the complexity of the domain structure, but a steeply falling field gradient is expected above the surface. The high surface field and the strong gradient of the magnetic field above the surface make it a good candidate for the atom mirror. Since the reflectivity of cold atoms from the (100) film is expected to be sensitive to small external magnetic fields, studies on the domain dynamics and domain relaxation are possible. Our method offers a unique measurement of certain properties of these films that are of interest in condensed-matter physics, and this was the motivation for conducting the atomic-reflection experiment with LCMO films.

5.1 Magnetic phase transition of LCMO

The magnetic phase transition was observed by measuring the reflectivity of cold atoms from the LCMO thin-film atom mirror at different temperatures. The spin-polarised cold atoms were dropped on the film from a height of 17 mm and the TOF signals of the atoms bouncing from the mirror were observed at different temperatures. The ratio of the absorption signals during reflection and fall gives a direct measurement of the reflectivity at different temperatures. The temperature dependence of the reflectivity is shown in Figure 16 and clearly shows the magnetic phase transition at 250 K. This may be compared with the magnetisation of the film measured in the SQUID magnetometer at different temperatures in the presence of a magnetic field of 1000 G, applied parallel to the surface. The behaviour of the phase transition in both cases is similar, but the reflectivity curve saturates faster than the curve measured using the SQUID magnetometer.

5.2 Domain relaxation

The domain relaxation in the LCMO thin film was studied in our atomic-reflection experiment. A magnetic field of about 200 Gauss was applied parallel to the surface of the LCMO thin film for a few minutes. After switching off the applied magnetic field, the spin-polarised cold atoms were dropped several times in order to observe the reflection of the atoms from the film over a time scale of 300 minutes, so as to track the domain relaxation. The change in the reflectivity with time is shown in Figure 17, and the observed increase of reflectivity is linked to a slow change in the domain characteristics. The reflectivity as a function of domain relaxation can be modelled by considering the competition between the attractive atom-surface interaction and the change in the range of the repulsive magnetic interaction due to the relaxation of the domains. However, the complexity of the domain pattern of the LCMO thin film makes it difficult to model the change in the range of the repulsive magnetic interaction potential. Nevertheless, it seems reasonable to suggest, based on the experimental data shown in Figure 17, that the change in reflectivity is related to the relaxation of the domains and perhaps to a growth in their size, while retaining a quasi-periodic structure. If that is the case, the mean distance from which the atoms are reflected increases, and the attractive atom-surface interaction decreases, resulting in the reflectivity slowly increasing with time. Another possibility that does not involve the competition from the attractive force is the emergence of the quasi-periodic structure from a relatively smooth, large domain — then the gradient of the magnetic potential becomes steeper in time, and the reflectivity increases correspondingly. The long relaxation time is perhaps surprising, and should be treated as tentative, since the general behavior of relaxation is found to be sample-dependent and not reliably reproducible. Such

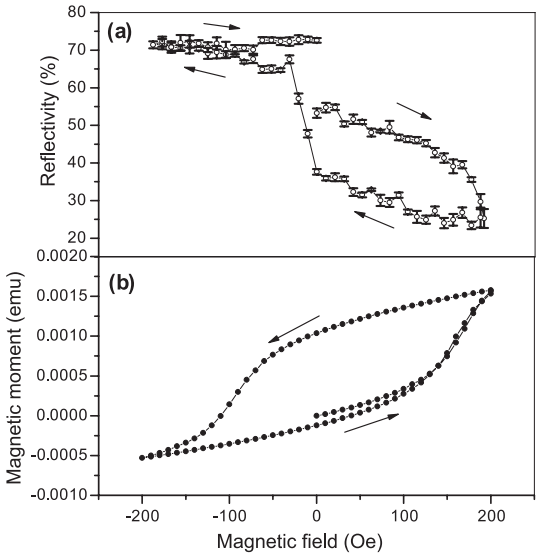

Fig. 18. (a) Reflectivity as a function of magnetic field applied parallel to the film's surface, and (b) the corresponding hysteresis measurement in the SQUID magnetometer.

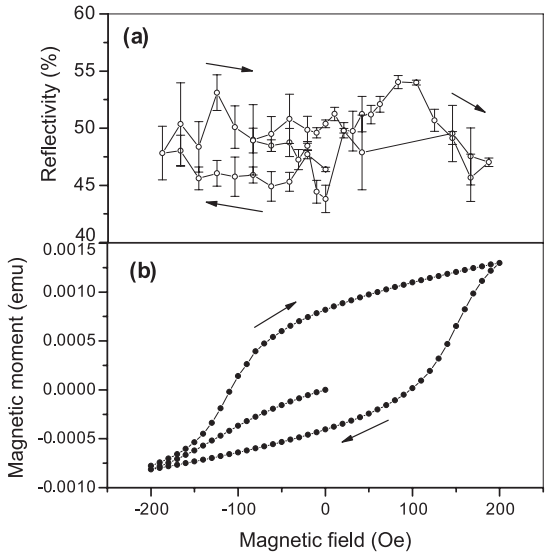

Fig. 19. (a) Reflectivity as a function of magnetic field, when the applied field is initially in the opposite direction to that in Figure 18, and (b) the corresponding hysteresis measurement in the SQUID magnetometer.

measurements are not available from condensed-matter experiments for a direct comparison.

5.3 Hysteresis measurement

Detailed measurements were undertaken to study the magnetic hysteresis of the thin film. A magnetic field was applied in steps of 10 G up to 200 G in one direction parallel to the plane of the film's surface. For each reading, the field was switched off and the reflectivity was measured within a few seconds. After reaching the value of 200 G (limited by the maximum current in the external coils, and the need to keep the vacuum chamber relatively non-magnetised for performing optical molasses), the field was reversed and the measurement was performed as when taking a typical hysteresis measurement, albeit at a very slow rate. The reflectivity as a function of the applied field is shown in Figure 18, where the direction of the field is also shown. The corresponding hysteresis measurement taken using the SQUID magnetometer is also shown in Figure 18. We do expect a reduction in the reflectivity as the field is increased, if the domains align together, merge, and grow large enough to reduce the gradient of the repulsive magnetic potential. Note that the SQUID magnetometer measures the magnetic moment as a function of the applied field, whereas atom reflectivity is indicative of the value of the gradient of the magnetic field above the surface of the film. The gradient decreases as the domains align together to form very large single domains, even though the magnetisation along the applied field increases. The hysteresis in this process explains the slow rise of the reflectivity as the field is reversed. The behaviour in the field range (-10 to 10 G) is surprising, with no corresponding behaviour in the SQUID-magnetometer measurement. A jump in the reflectivity is observed, and then the reflectivity remains more or less constant. It is as if a sudden, catastrophic change has taken place in the magnetic domain structure, causing the gradient of the magnetic field above the surface to increase sharply, reflecting most of the atoms. Note that the reflectivity after the jump is about 50% higher than the equilibrium value that we started with. An interesting possibility is the sudden break-up of the large domains into smaller quasi-periodic ones. This has to be spontaneous rather than field-driven, because the sudden change was observed when the applied field was close to zero.

A similar measurement was performed on the same film, with the initial direction of the field opposite to that of the previous measurement. The reflectivity as a function of the applied field for this measurement is shown in Figure 19. The corresponding hysteresis measurement in the SQUID magnetometer is also shown in the figure. There is a large asymmetry observed between this data and the data obtained with the initial direction of the field applied opposite, as in the previous measurement. Much less asymmetry is observed when the measurements are taken using the SQUID magnetometer, even though the hysteresis curves are not identical. However, there are features seen in the reflectivity experiment that are not revealed in the SQUID measurement. Some of these features may depend on the history of the film, preparation method, etc., and more experiments are required before definite and general conclusions on the physics of domain structures can be drawn. From these preliminary results, it is clear that study of the magnetic behaviour of the thin films at a microscopic level is possible in measurements using ultra-cold atoms, opening up new possibilities in the study of thin-film magnetic surfaces. At present, such studies might seem tedious compared to the conventional measurements. However, since the cold atoms

probe an area corresponding to only a few domains at the 100-nanometer scale, these measurements are unique and can be important in specific cases.

6 Conclusion

We have studied the reflection of cold atoms from a new type of atom mirror made of ferromagnetic thin films of cobalt and LCMO. The cobalt thin-film atom mirrors have high reflectivity when the thickness of the film is larger than about 200 nanometers, but they are not as smooth as the ones made from magnetic videotapes etc., because the atoms approach very close to the surface of the thin film before they are reflected. However, this kind of mirror is well-suited for precision measurement of the atom-surface interaction. The reflectivity of the atoms depends on the thickness of the thin films. By measuring the reflectivity of the cold atoms from cobalt thin films of different thicknesses, the van der Waals force on a rubidium atom in its ground state near a conducting surface is determined with an uncertainty of 15%. The magnetic phase transition, as well as several interesting features of the domain relaxation and dynamics in the LCMO thin film, are observed in the atomic-reflection experiments, pointing to the possibility of new microscopic measurements of interest to condensed-matter studies.

We thank P. Raychowdhury, G. Sheet, V. Bagwe, S.C. Purandare, and S.K. Gohil for their help with the cobalt thin films. We thank P.G. Rodrigues and Simon Pereira for help with electronics, and S. Guram for help with mechanical assembly. We thank H.M. Antia for fruitful discussions on data analysis.

References

1. A.K. Mohapatra, C.S. Unnikrishnan, Europhys. Lett. **73**, 839 (2006)
2. A.K. Mohapatra, Ph.D. thesis, Tata Institute of Fundamental Research (2005), available at `http://www.tifr.res.in/~filab`
3. M.A. Kasevich, D.S. Weiss, S. Chu, Opt. Lett. **15**, 607 (1990)
4. C.G. Aminoff, A.M. Steane, P. Bouyer, P. Desbiolles, J. Dalibard, C. Cohen-Tannoudji, Phys. Rev. Lett. **71**, 3083 (1993)
5. S. Feron, J. Reinhardt, S. Le Boiteux, O. Gorceix, J. Baudon, M. Ducloy, J. Robert, Ch. Miniatura, S. Nic Chormaic, H. Haberland, V. Lorent, Opt. Comm. **102**, 83 (1993)
6. G.I. Opat, S.J. Wark, A. Cimmino, Appl. Phys. B **54**, 396 (1992)
7. E.A. Hinds, I.G. Hughes, J. Phys. D: Appl. Phys. **32**, R119 (1999)
8. A. Landragin, Y. Courtois, G. Labeyrie, N. Vansteenkiste, C.I. Westbrook, A. Aspect, Phys. Rev. Lett. **77**, 1464 (1996)
9. T.M. Roach, H. Abele, M.G. Boshier, H.L. Grossman, K.P. Zetie, E.A. Hinds, Phys. Rev. Lett. **75**, 629 (1995)
10. I.G. Hughes, P.A. Barton, T.M. Roach, M.G. Boshier, E.A. Hinds, J. Phys. B: At. Mol. Opt. Phys. **30**, 647 (1997)
11. C.V. Saba, P.A. Barton, M.G. Boshier, I.G. Hughes, P. Rosenbusch, B.E. Sauer, E.A. Hinds, Phys. Rev. Lett. **82**, 468 (1999)
12. A.I. Sidorov, R.J. McLean, W.J. Rowlands, D.C. Lau, J.E. Murphy, M. Walkiewicz, G.I. Opat, P. Hannaford, J. Opt. B: Quantum semiclass. Opt. **8**, 713 (1996)
13. D.C. Lau, A.I. Sidorov, G.I. Opat, R.J. McLean, W.J. Rowlands, P. Hannaford, Eur. Phys. J. D **5**, 193 (1999)
14. P. Rosenbusch, J.A. Retter, B.V. Hall, E.A. Hinds, F. Lison, D. Haubrich, D. Meschede, Appl. Phys. B **70**, 661 (2000)
15. M. Drndić, K.S. Johnson, J.H. Thywissen, M. Prentiss, R.M. Westervelt, Appl. Phys. Lett. **72**, 2906 (2006)
16. A.I. Sidorov, R.J. McLean, F. Scharnberg, D.S. Gough, T.J. Davis, B.A. Sexton, G.I. Opat, P. Hannaford, Acta Phys. Pol. B **33**, 2137 (2002)
17. A.K. Mohapatra, C.S. Unnikrishnan, Pramana-J. Phys. **66**, 1027 (2006)
18. M. Hehn, S. Padovani, K. Ounadjela, J.P. Bucher, Phys. Rev. B **54**, 3428 (1996)
19. A. Corney, *Atomic and Laser Spectroscopy* (Clarendon Press, Oxford, 1997)
20. G.I. Opat, S. Nic Chromaic, B.P. Cantwell, J.A. Richmond, J. Opt. B: Quantum Semiclass. Opt. **1**, 415 (1999)
21. C. Kittel, Phys. Rev. **70**, 965 (1946)
22. É. Maréchal, S. Guibal, J.L. Bossennec, M.P. Gorza, R. Barbé, J.C. Keller, O. Gorceix, Eur. Phys. J. D **2**, 195 (1998)
23. A. Derevianko, W.R. Johnson, M.S. Safronova, J.F. Babb, Phys. Rev. Lett. **82**, 3589 (1999)
24. J. Mitroy, M.W.J. Bromley, Phys. Rev. A **68**, 052714 (2003)
25. M. Liebmann, U. Kaiser, A. Schwarz, R. Wiesendanger, U.H. Pi, T.W. Noh, Z.G. Khim, D.W. Kim, J. Appl. Phys. **93**, 8319 (2003)
26. S. Valencia, Li. Balcells, B. Martinez, J. Fontcuberta, J. Appl. Phys. **93**, 8059 (2003)
27. S.H. Chung, S.R. Shinde, S.B. Ogale, T. Venkatesan, R.L. Greene, M. Dreyer, R.D. Gomez, J. Appl. Phys. **89**, 6784 (2001)